

# Forward-Looking Volumetric Intracardiac Imaging Using a Fully Integrated CMUT Ring Array

Amin Nikoozadeh<sup>1</sup>, Ömer Oralkan<sup>1</sup>, Mustafa Gencel<sup>1</sup>, Jung Woo Choe<sup>1</sup>, Douglas N. Stephens<sup>2</sup>, Alan de la Rama<sup>3</sup>, Peter Chen<sup>3</sup>, Kai Thomenius<sup>4</sup>, Aaron Dentinger<sup>4</sup>, Douglas Wildes<sup>4</sup>, Kalyanam Shivkumar<sup>5</sup>, Aman Mahajan<sup>5</sup>, Matthew O'Donnell<sup>6</sup>, David Sahn<sup>7</sup> and Pierre T. Khuri-Yakub<sup>1</sup>,

1 Stanford University, 2 University of California, Davis, 3 St. Jude Medical, 4 General Electric Corporate Research & Development, 5 University of California, Los Angeles, 6 University of Washington, 7 Oregon Health and Science University

e-mail: aminn@stanford.edu

**Abstract** — Atrial fibrillation is the most common type of cardiac arrhythmia that now affects over 2.2 million adults in the United States alone. Currently fluoroscopy is the most common method for guiding interventional electrophysiological procedures. We are developing a 9-F forward-looking intracardiac ultrasound catheter for real-time volumetric imaging. We designed and fabricated a 64-element 10-MHz CMUT ring array with through-wafer via interconnects. We also designed custom front-end electronics to be closely integrated with the CMUT array at the tip of the catheter for improved SNR. This integrated circuit (IC) is composed of preamplifiers and protection circuitry, and can directly interface a standard imaging system. This multi-channel IC is capable of passing up to  $\pm 50$ -V bipolar pulses. An 8-channel front-end IC was fabricated based on this circuit topology. Additionally, a flexible PCB was designed for the integration of ring array with front-end electronics. We have acquired a PC-based real-time imaging platform and demonstrated real-time imaging with the ring array. We have also shown volume images using off-line full synthetic aperture image reconstruction method. The presented experimental results demonstrate the performance of our forward-looking volumetric intracardiac imaging approach. We are currently working on the final catheter integration and further development of our real-time imaging methods.

**Keywords** – *electrophysiology; intracardiac echo; real-time; volumetric; forward-looking; ultrasound; capacitive micromachined ultrasonic transducers; CMUT*

## I. INTRODUCTION

Atrial fibrillation, the most common sustained type of arrhythmia, now affects over 2.2 million adults in the United States alone with over 60,000 new cases each year [1]. Currently fluoroscopy is the most common guidance method in electrophysiological (EP) interventions. However, the ionizing radiation of fluoroscopy has been shown to be dangerous for both the patient and the physician. Also fluoroscopy does not provide good soft tissue resolution, even in the presence of contrast agents. Intracardiac echo (ICE) imaging has proven

useful in improving visualization and reducing the exposure time to fluoroscopy [2].

In this effort we are developing a 9-F ring catheter for real-time forward-looking volumetric intracardiac imaging. The ring catheter is an ICE imaging catheter designed for use in EP interventions. This catheter is a multifunction device with a CMUT ring array at the catheter tip for real-time, forward-looking, volumetric imaging (Fig. 1). The ring geometry provides a lumen in the center of the catheter that may be utilized for a variety of applications such as radio-frequency (RF) ablation, laser ablation, photo-acoustic imaging, etc. A short description of the components of the ring catheter and their method of integration is provided in this paper. Also some early imaging results with the ring array are shown.

## II. METHODS

### A. CMUT Array Design

The fabricated CMUT ring array dimensions are summarized in Table I.

TABLE I. CMUT RING ARRAY DESIGN PARAMETERS

Array Design Parameters	
<i>Number of elements</i>	64
<i>Center frequency (MHz)</i>	10
<i>Array pitch (<math>\mu\text{m} \times \mu\text{m}</math>)</i>	$80 \times 100$
<i>Outer diameter (mm)</i>	2.54
<i>Outer diameter</i>	1.63
Cell Design Parameters	
<i>Membrane thickness (<math>\mu\text{m}</math>)</i>	0.50
<i>Gap height (<math>\mu\text{m}</math>)</i>	0.10
<i>Insulator layer thickness (<math>\mu\text{m}</math>)</i>	0.18

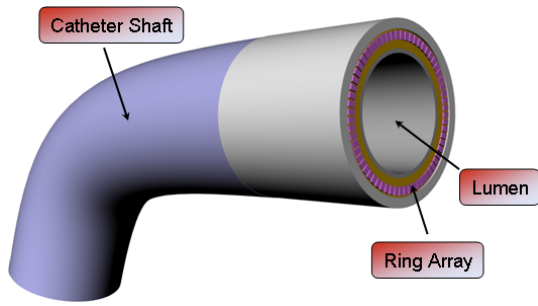


**Figure 1.** Conceptual drawing of the ring catheter.

The ring array is a 64-element array with the transducer elements distributed along the periphery of the device. This device was fabricated using the standard poly-silicon sacrificial layer process with electrical through-wafer interconnects [3]. These vias connect the individual signal electrodes and the common reference electrode to the flip-chip bond pads on the back side of the array. Fig. 2 shows an optical picture of an array with rectangular membranes with 18- $\mu\text{m}$  width. The singulation of the arrays and also the fabrication of the inner hole were performed using a single step deep reactive ion etching process.

### B. Custom-Designed Front-End Electronics

Each element of the CMUT ring array has a capacitance of less than 1 pF, which is quite small compared to the cable capacitance of about 200 pF in a typical catheter assembly. Direct connection of these small elements to the imaging system may result in poor image quality. Fig. 3 shows the simulation result of noise figure (NF) when the ring element is directly connected to an imaging system with a coaxial cable. In these simulations the coaxial cable was assumed loss-less. The cable loss will degrade the noise figure even further.

We designed an application-specific integrated circuit (ASIC) to improve the performance of the overall system. The top-level block diagram of a single transmit/receive (TX/RX) channel for this ASIC is shown in Fig. 4. This circuit architecture enables seamless integration with the imaging system as it uses only a single cable per TX/RX channel. The circuit is divided into two paths: the transmit path on top allows the transmit signal from the imaging system to pass through. The diode expander circuitry in the transmit path provides an open-circuit for this path when in receive mode. The bottom

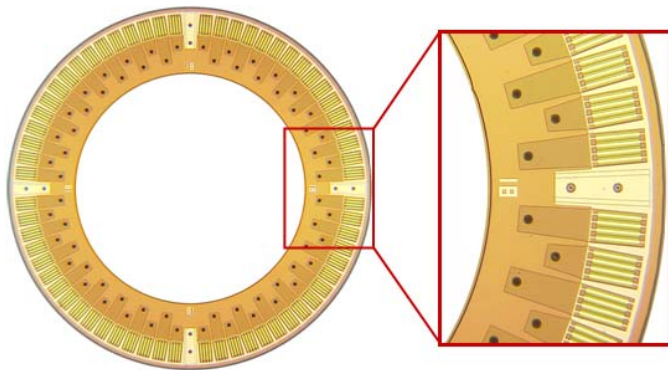


**Figure 2.** Optical picture of a CMUT ring array composed of rectangular membranes.

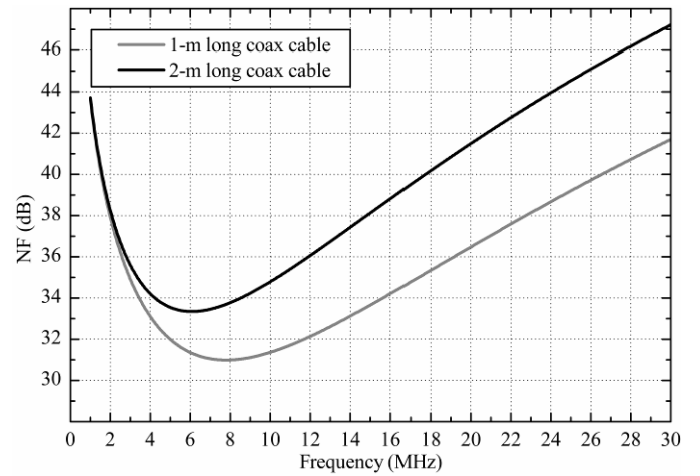


**Figure 3.** NF simulation results of the direct connection of the ring array element to a typical imaging system using 1 and 2-m long coaxial cables (coaxial cable's parameters:  $C = 104$  pF/m,  $L = 220$  nH/m,  $R = 0$   $\Omega$ /m, imaging system's parameters:  $I_{n,in} = 6$  pA/ $\sqrt{\text{Hz}}$ ,  $V_{n,in} = 0.78$  nV/ $\sqrt{\text{Hz}}$ ).

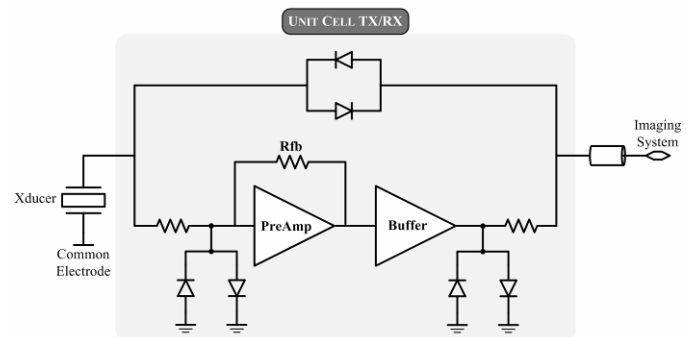


**Figure 4.** Top-level block diagram of the circuit.

path is the receive path and it provides a low-noise preamplifier and a buffer. The preamplifier is a transimpedance amplifier with a gain of 50 k $\Omega$ . Both the input and output of the receive path is protected from high-voltage pulses using diode limiters. The simulation result shown in Fig. 5 indicates a 15-20 dB improvement in NF of the system with the addition of this ASIC. Fig. 5 also points out some of the main noise contributors of the circuit. The feedback resistor in the preamplifier is the largest contributor to the noise. This resistor is formed using a transistor-type structure and it has an additional noise component other than the thermal noise. If the process provides, for example, an un-doped poly resistor the noise figure can be improved as shown in Fig. 5.

This ASIC was designed in an 8-channel configuration (Fig. 6). A total of 8 IC's are required to address the 64 elements of the ring array.

### C. Real-time Imaging

We have acquired a PC-based imaging system (VeraSonics, Inc., Redmond, WA) for real-time imaging. RF data acquired in the system's hardware is transferred to the host computer memory. Digital image processing is then performed and the image is displayed on computer's display.

We are currently working on several real-time image reconstruction schemes: flash imaging (flat transmit, beamforming on receive), phased array imaging (beam steering and focusing), and full synthetic phased array imaging.

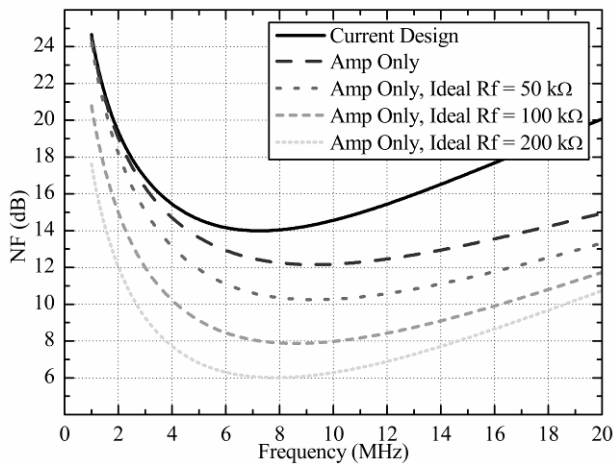


**Figure 5.** NF plots. Solid line shows the NF simulation results when the ASIC is placed between the ring element and a 1-m coaxial cable that is connected to the imaging system (coaxial cable’s parameters:  $C = 104$  pF/m,  $L = 220$  nH/m,  $R = 30$   $\Omega$ /m, imaging system’s parameters:  $I_{n,in} = 6$  pA/ $\sqrt{\text{Hz}}$ ,  $V_{n,in} = 0.78$  nV/ $\sqrt{\text{Hz}}$ ). The other graphs illustrate the contribution of the protection circuitry to the NF and also the effect of feedback resistor (Amp Only: only the preamp and the buffer).

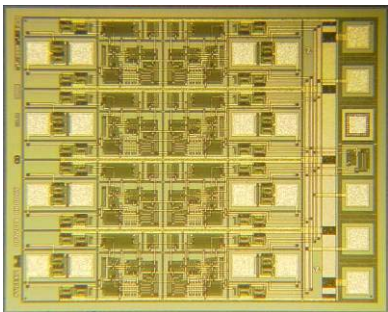


**Figure 6.** Die photograph.

To develop our real-time imaging, 8 ASIC’s were wire-bonded to a ring array in a pin grid array package. An interface box was also designed to interface the ring assembly to the imaging system.

### III. RESULTS

#### A. Array and ASIC Characterization

The ring-ASIC assembly was used to characterize the performance of the ring array and the ASIC. We measured the pulse-echo response of an element of the ring array from a plane reflector (oil-air interface) [Fig. 7]. Also the acoustic pressure generated by a ring array element was measured at two DC biases with various input pulse amplitudes (Fig. 8).

#### B. Imaging Tests

We demonstrated real-time imaging using flash and conventional phased array imaging methods. The preliminary real-time imaging results proved promising and we are continuing to further develop these and other imaging methods.

We also acquired the full set of  $64 \times 64$  RF data for two imaging phantoms for off-line synthetic phased array image

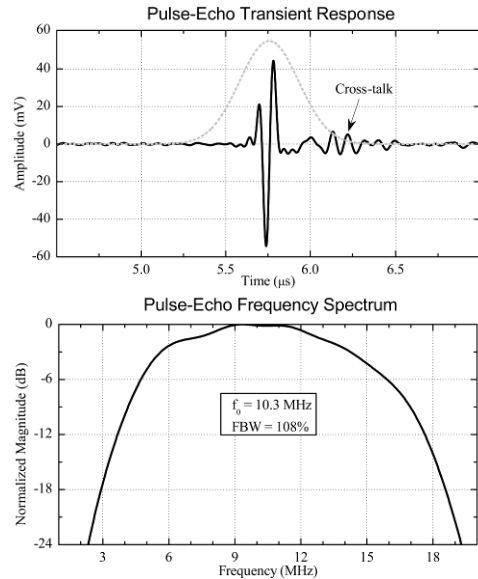


**Figure 7.** Pulse-echo response and the corresponding frequency spectrum. Ring array was biased at -45 VDC and a single cycle bipolar pulse with an amplitude of  $\sim 40$  Vp-p was applied.

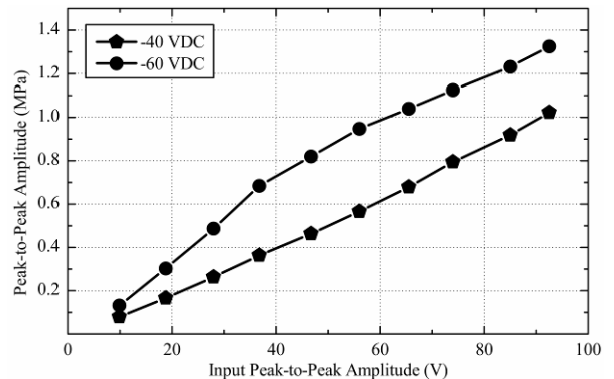
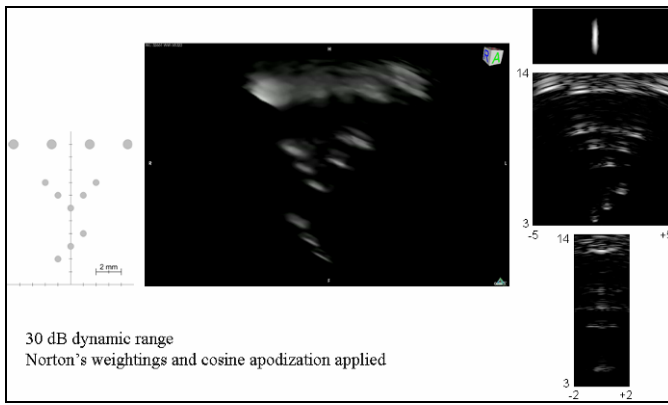


**Figure 8.** Acoustic pressure at the face of a ring element. A 10-cycle, tone-burst with an increasing amplitude was applied. Pressure was measured using a calibrated hydrophone and then corrected for attenuation and diffraction losses.

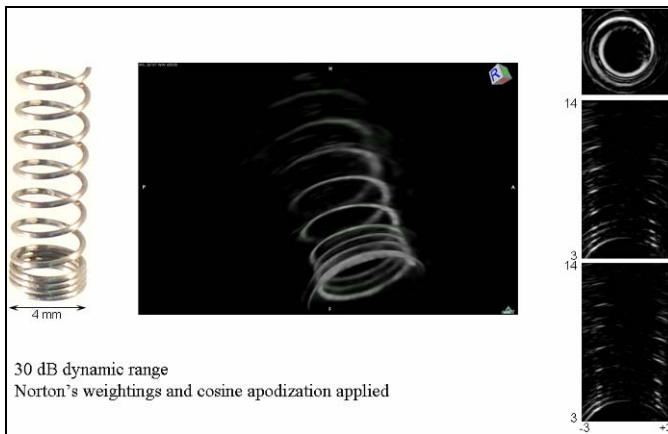
reconstruction (Fig. 9). Fig. 9a shows the volume-rendered image of nylon wires and Fig. 9b shows the volume-rendered image of a metal spring. For both images Norton’s weightings for full-aperture resolution [4] and cosine apodization were applied, same way as explained in [5].

### IV. CATHETER ASSEMBLY

A flexible PCB (flex) was designed and fabricated that is composed of 8 long and narrow legs that intersect at the center of the flex. The ring array is flip-chip bonded to the center of the flex and one IC is flip-chip bonded to each leg to address a total of 64 channels (Fig. 10). The flex legs are then folded around the ring array for cabling and final integration with the catheter shaft. The cables are first laced into the catheter shaft and then terminated on the flex legs. Finally the cables are pulled into the catheter shaft and the catheter is finalized.



(a)



(b)

**Figure 9.** Off-line images reconstructed using synthetic phased array imaging method. In each panel, the center image shows the volume-rendered image and the right images show the cross-sectional images (dimensions in mm). (a) Nylon wire phantom as shown in the left hand side. (b) metal spring as shown

Fig. 11 shows a ring flex assembly before cable attach. It also shows a mock-up of the ring catheter, which was assembled with a ring-flex assembly.

## V. CONCLUSIONS

We have designed and tested all the components of the CMUT ring catheter. The successful integration of the ring array and the ASIC's was demonstrated. The preliminary imaging results also demonstrated the functionality and the performance of all the system components integrated together.

Currently we are continuing to work on the real-time image processing. Also the final catheter assembly, which includes cable attachment and final catheter assembly, is underway.

## ACKNOWLEDGMENT

This work was funded by the National Institutes of Health under grant 5R01HL067647. We would like to thank National Semiconductor (Santa Clara, CA) for their valuable support in the design and fabrication of the IC. CMUT fabrication was done at the Stanford Nanofabrication Facility (Stanford, CA), which is a member of National Nanotechnology Infrastructure Network. Solder bumping was provided by Pac Tech USA Inc.

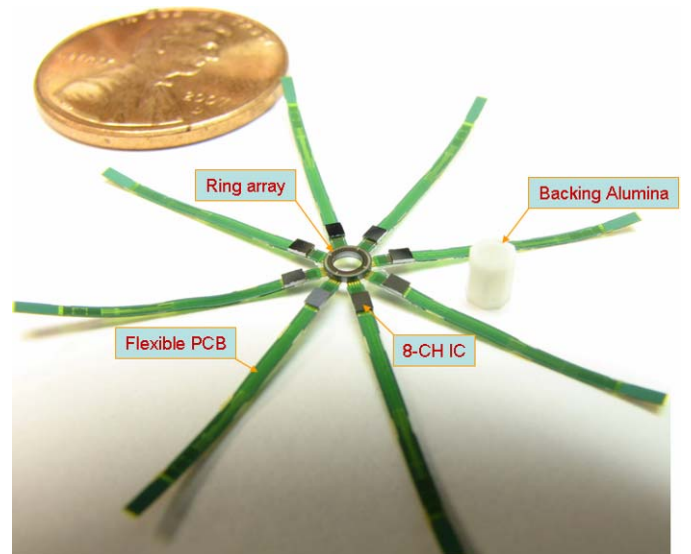


**Figure 10.** A ring flex assembly after flip-chip bonding the ring array and 8 IC's.

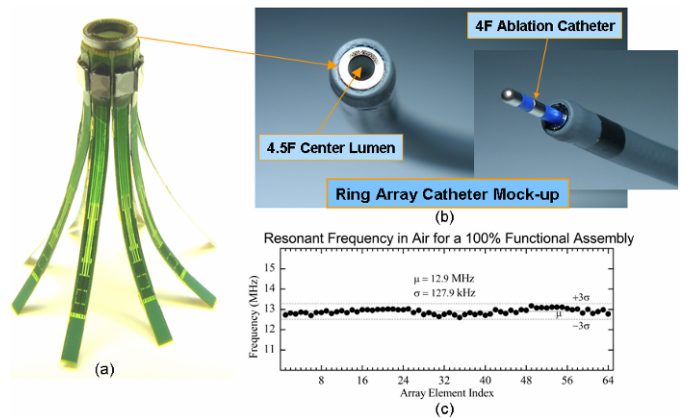


**Figure 11.** (a) A completed ring assembly ready for cable attachment and integration with catheter shaft. (b) a catheter mock-up showing how the catheter shaft is integrated with the ring assembly. (c) resonant frequency in air for all the 64 elements of a ring flex assembly confirming that the assembly is fully functional.

(Santa Clara, CA). We also thank VeraSonics for their programming support

## REFERENCES

- [1] Go AS, Hylek EM, Phillips KA, et al., "Prevalence of diagnosed atrial fibrillation in adults: national implications for rhythm management and stroke prevention: the anticoagulation and risk factors in AF (ATRIA) study," *JAMA*, vol. 285, pp. 2370-5, 2001.
- [2] M. Jongbloed, M. Schalij, K. Zeppenfeld, P. Oemrawsingh, E. van der Wall, J. Bax, "Clinical applications of intracardiac echocardiography in interventional procedures," *Heart*, vol. 91, pp. 981-990, 2005.
- [3] A. S. Ergun, Y. Huang, X. Zhuang, O. Oralkan, G. G. Yarahoglu, B. T. Khuri-Yakub, "Capacitive micromachined ultrasonic transducers: fabrication technology," *IEEE Trans. Ultrason., Ferroelect., Freq. Contr.*, vol. 52, no. 12, pp. 2242 - 2258, Dec. 2005.
- [4] S. J. Norton, "Annular array imaging with full-aperture resolution," *J. Acoust. Soc. Am.*, vol. 92, no. 6, pp. 3202-3206, Dec. 1992.
- [5] D. T. Yeh, O. Oralkan, I. O. Wygant, M. O'Donnell, and B. T. Khuri-Yakub, "3-D ultrasound imaging using a forward-looking CMUT ring array for intravascular/intracardiac applications," *IEEE Trans. Ultrason., Ferroelect., Freq. Contr.*, vol.53, no.6, pp. 1202- 1211, June 2006.